# Polymer Chemistry

Accepted Manuscript






ROYAL SOCIETY OF CHEMISTRY

www.rsc.org/polymers

Polymer Chemistry

RSCPublishing

ARTICLE

# Doubly Responsive Polymersomes towards Monosaccharides and Temperature under Physiologically Relevant Conditions

Cite this: DOI: 10.1039/x0xx00000x

Received 00th January 2012,
Accepted 00th January 2012

DOI: 10.1039/x0xx00000x

www.rsc.org/

Eun Sun Jeong,[a] Chiyoung Park*[a] and Kyoung Taek Kim*[a]

Organoboronic acid-containing polymers and block copolymers have attracted recent attention because of their ability to recognize important natural diol compounds such as saccharides and nucleotides under physiologically relevant conditions at neutral pH. In particular, polymers and block copolymers that are responsive toward multiple stimuli can be utilized to create smart delivery vehicles for use in applications in complex environment. Here we report the monosaccharide-responsive polymers and block copolymers comprised of styreneboroxole and oligo(ethylene glycol)-functionalized styrenes (OEG-STs) as repeating units. We show that homopolymers and copolymers of OEG-STs are thermally responsive by demonstrating that they possess the characteristic of tunable lower critical solution temperature (LCST) in water. When copolymerized with OEG-STs, styreneboroxole units function as a switch to change the solubility of the resulting polymers in aqueous solution by recognizing monosaccharide via formation of boronate ester. By introducing the minimum number of monosaccharide-responsive styreneboroxole units onto the thermally responsive OEG-ST backbone consisting, we demonstrated the monosaccharide-responsive behavior of the resulting copolymers and their amphiphilic block copolymers in aqueous solution at physiologically relevant pH and temperature. A strategy based on doubly responsive block copolymers reported here could be utilized as new delivery vehicles for cargo molecules such as insulin, due to their ability to function in vivo environment.

## Introduction

Stimuli-responsive block copolymers that can self-assemble into compartmentalized nanostructures such as micelles and polymer vesicles (polymersomes) are attractive smart materials for creating delivery vehicles that regulate their release behavior in response to environmental changes.[1–5] In particular, stimuli-responsive polymersomes have attracted considerable attention because of their ability to deliver water-soluble cargo molecules triggered by external stimuli such as pH and temperature, as well as by the presence of biologically important molecules and their concentrations.[6–16] Polymers and block copolymers showing responsiveness toward multiple physical and chemical stimuli would be ideal for generating the delivery vehicles with release behavior that can be self-regulated in accordance with the external stimuli.[17,18] Such block copolymers would enable the resulting self-assembled nanostructures to regulate their behavior in response to changes in complex local environments in vivo.[19-25]

Organoboronic acid-containing polymers and block copolymers have attracted recent attention because of their ability to recognize important natural diol compounds such as saccharides and nucleotides.[26-31] The formation of reversible covalent bonds between organoboronic acid and various diol compounds has also been utilized to create sensors, drug delivery systems and hydrogels, as well as in sensing and molecular computing.[32-54] Among the diols that bind to boronic acid, the monosaccharide glucose is particularly important due to its relevance to human diseases such as diabetes.[55-59]

We have studied organoboronic acid-containing polymers as macromolecular receptors for monosaccharides such as glucose and fructose.[60,61] In comparison with phenylboronic acids,[49-51] benzoboroxole derivatives have shown higher binding affinities toward pyranose-form monosaccharides and non-reducing sugars under physiological pH. We synthesized a styrenic derivative of benzoboroxole, styreneboroxole (**StB** in Scheme 1), with the capacity to be polymerized into well-defined polymers and block copolymers by reversible addition–fragmentation chain transfer (RAFT) polymerization.[60] The resulting poly(styreneboroxole) (PBOx) exhibited monosaccharide-responsive solubility change in aqueous buffer at neutral pH. When PBOx was conjugated with a water-soluble poly(ethylene glycol) (PEG) block, the resulting monosaccharide-responsive block copolymers (PEG-*b*-PBOx) exhibited self-assembly behavior analogous to that of conventional amphiphilic block copolymers in water. PEG-*b*-PBOx self-assembled into polymersomes in aqueous solution, which demonstrated monosaccharide-responsive disassembly due to changes in the solubility of the PBOx block in water caused by the binding of monosaccharide into benzoboroxole units.[62-64] These

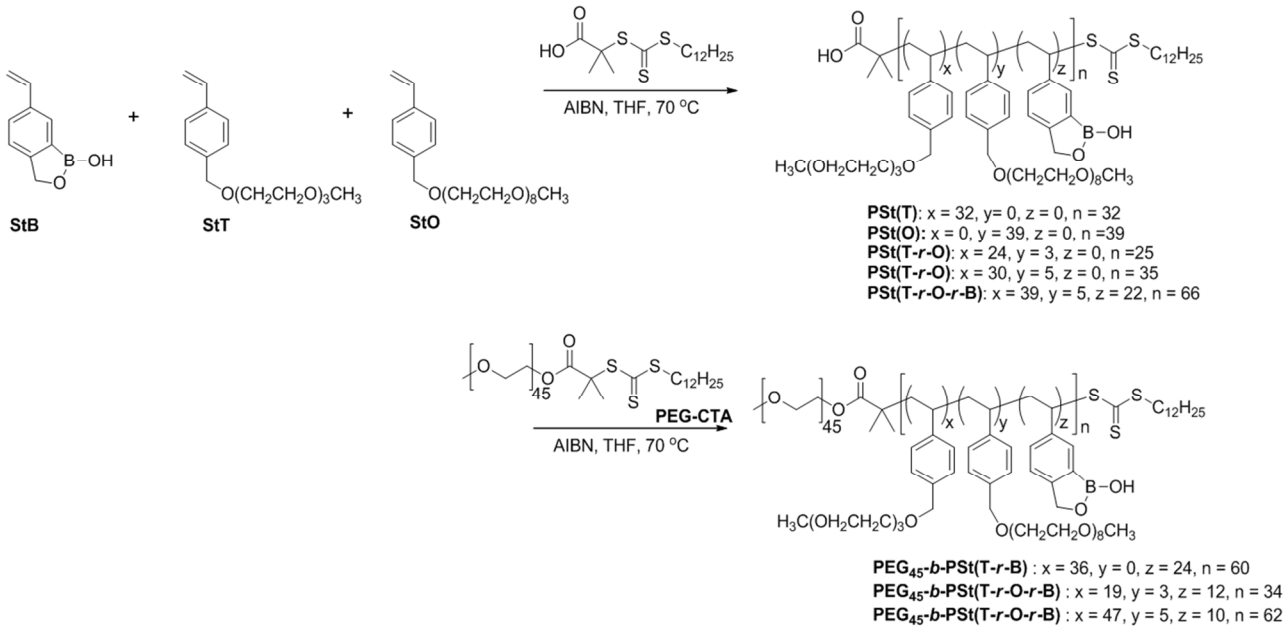


**Scheme 1** Synthesis of terpolymers and block copolymers of styreneboroxole and styrenic oligo(ethylene glycol)s by the RAFT polymerization.

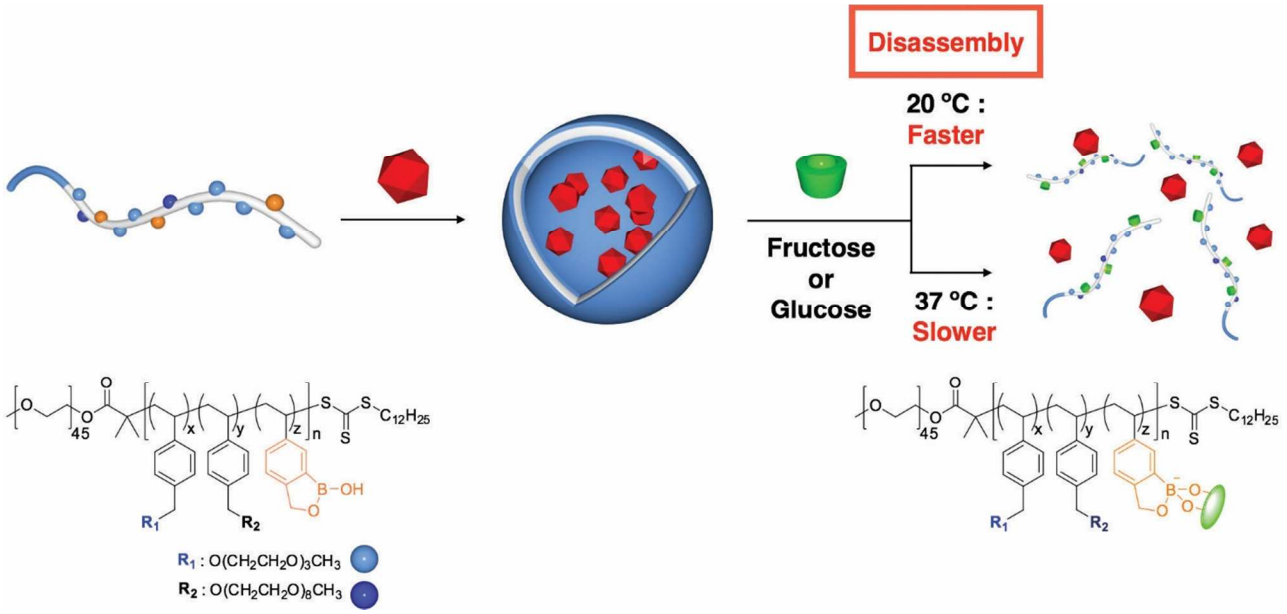


**Figure 1** Schematic illustration for self-assembly of sugar- and thermo-responsive block copolymers and their disassembly in the presence of monosaccharides.

polymersomes enabled the release of encapsulated cargo molecules such as insulin, to be triggered by the presence of glucose under physiologically relevant condition.[60]

Here we report new monosaccharide-responsive benzoboroxole-containing polymers and block copolymers that are comprised of **StB** and oligo(ethylene glycol)-functionalized styrenes (OEG-STs) (Figure 1). We show that homopolymers and random copolymers of OEG-STs are thermally responsive by demonstrating that they possess the characteristic of tunable lower critical solution temperature (LCST) in water. **StB** units function as a switch to change the solubility of the copolymers in aqueous solution by recognizing monosaccharides via the formation of boronate ester. By introducing the minimum number of the monosaccharide-responsive **StB** units onto the thermally responsive OEG-ST backbone, we conferred the monosaccharide-responsive behavior on the resulting copolymers and their amphiphilic block copolymers in aqueous solution at physiologically relevant pH and temperature. This dual-responsive nature could allow the copolymers to be utilized in new delivery vehicles for water-soluble cargo molecules such as insulin, due to their ability to function in, and adapt to, in vivo environment.

## Experimental



 

### Synthesis of Polymers and Block Copolymers

Details of synthesis of OEG-STs and their homopolymers and copolymers of **StB** and OEG-STs, and block copolymers with a PEG-macro chain transfer agent and the characterization data for synthesized polymers are provided in Electronic Supplementary Information (ESI).

### Preparation of Polymersome Solution

Triply distilled water (Milli-Q, 18.2 MΩ) was used throughout the experiments. A typical procedure was as follows: the block copolymer **$PEG_{45}$-*b*-PSt($T_{47}$-*r*-$O_5$-*r*-$B_{10}$)** (2 mg) was dissolved in THF (1 mL) in a 15 mL capped vial with a magnetic stirrer. The solution was stirred for 15 min at room temperature. A syringe pump was calibrated to deliver water at a speed of 2.5 mL/h. The vial cap was replaced with a rubber septum, and 5 mL of water was added to the organic solution with vigorous stirring (850 rpm) by a syringe pump with a 5 mL syringe equipped with a steel needle. After the addition of water, the suspension was subjected to dialysis (SpectraPor, molecular weight cut-off: 12,000−14,000 Da) against water for 24 h with frequent changes of water. The resulting solution was collected from a dialysis bag. The diameter and morphology of the polymersomes were studied by dynamic light scattering (DLS) and transmission electron microscopy (TEM). When necessary, the medium was exchanged by repeated centrifugal filtrations (Amicon, Membrane cut-off: 100 kDa; 5000 rpm for 3 min), followed by dilution with phosphate buffer (HEPES, pH 7.5).

### LCST Measurement

The cloud points of the polymers ~~solutions~~ (3 mg/ml in distilled water) were measured on an Agilent 8453 UV-vis spectrophotometer. The transmittance of the solutions at 580 nm was monitored as a function of temperature (cell path length: 1 cm).

### LCST Measurement. Turbidity Test of the Polymersome Solutions

The pH of the polymersome solution was adjusted to 7.5 by adding aqueous NaOH (1 M). Before the measurement, the polymersome solution (HEPES, pH 7.5) was charged in a quartz cuvette with a magnetic stir bar and equilibrated at the desired temperature. For the turbidity measurement, fructose or glucose stock solution (at the desired concentration) was added to the prepared polymersome solution. The transmittance at 580 nm was measured as a function of time with a constant stirring, and recorded using an Agilent 8453 UV-vis spectrophotometer. The transmittance (%) at 580 nm was used to calculate the optical transmittance (O.T) of the solution by the following equation. $O.T = 1 - ((T_{buf} - T_{sol})/T_{buf})$ where $T_{buf}$ was the percentage transmission of the buffer at 580 nm and $T_{sol}$ was the % transmittance of the solution at the same wavelength.

### The Encapsulation of Rhodamine B in the Polymersomes

The block copolymer **$PEG_{45}$-b-PSt($T_{47}$-*r*-$O_5$-*r*-$B_{10}$)** (2 mg) was dissolved in THF (1 mL) in a 15 mL capped vial with a magnetic stirrer, and the solution was stirred for 15 min at room temperature. A syringe pump was calibrated to deliver water at a speed of 2.5 mL/h. The vial cap was replaced with a rubber septum. 5 mL of water having Rhodamine B (1 mM) was added to the organic solution with vigorous stirring (850 rpm) by a syringe pump with a 5 mL syringe equipped with a steel needle. After the addition of water, the suspension was subjected to dialysis (SpectraPor, molecular weight cut-off: 12,000−14,000 Da) against water for 3 days with frequent changes of water. The resulting solution was collected from a dialysis bag, and passed through a size-exclusion column (Sephadex G-100) to remove unencapsulated Rhodamine B using water as an eluent. The resulting polymersome solution was used in the release experiments and the confocal laser scanning microscopy analysis.

### Preparation and Analysis of Confocal Laser Scanning Microscopy Samples

The solution of the polymersomes with the encapsulated Rhodamine B dye was transferred onto a slide glass and quickly sealed with a coverslip to avoid drying of the sample. The confocal fluorescence images were taken directly with FV1000 laser confocal fluorescence microscopy (Olympus). The images were viewed and processed with the FV1000 viewer software (Olympus). The emission of Rhodamine B at 580 nm was monitored with an excitation wavelength at 540 nm.

### Release of Encapsulated Dyes from Polymersomes.

The solution (1 mL) of the polymersome with encapsulated Rhodamine B dye was mixed with water (1 mL) in a fluorescence cuvette. The emission of Rhodamine B at 580 nm was monitored with an excitation wavelength at 540 nm. After the measurements were completed, 10 % Triton X-100 (20 μL) was added to lyse the polymersomes.
The dye release (%) was calculated using the following formula,
Release percentage (%) = $(I_t - I_0) / (I_\infty - I_0) \times 100$
where $I_0$ was the initial fluorescence intensity, It was the fluorescence intensity at time $t$ and $I_\infty$ was the maximum fluorescence intensity after the addition of the Triton X-100 solution.

## Results and Discussion

### Synthesis and Polymerization of Oligo(ethylene glycol)-Styrenes

Oligo(ethylene glycol)-functionalized styrenes were synthesized by reacting 4-vinylbenzyl chloride and sodium alkoxides of the corresponding monomethoxy oligo(ethylene glycol)s in THF (for synthetic details, see ESI and Figure S1). **StB** was synthesized according to a previously reported procedure.[60] 4-methoxy(triethylene glycol)methylether styrene (**StT**) and 4-methoxyoligo(ethylene glycol)methylether styrene (**StO**) (Scheme 1) were used as co- monomers to pair with **StB** for random copolymerization under RAFT polymerization conditions. First, we synthesized homopolymers of **StT** and **StO** to investigate their solution behavior in water. Under RAFT polymerization conditions with 2-(dodecylthiocarbonothioylthio)-2-methylpropionic acid as a chain transfer agent and azobisisobutyronitrile (AIBN) as a radical initiator (Scheme 1), both monomers showed linear increases in molecular weight over time (Figure S2). **StO** showed a polymerization rate slower than that of **StT** and the conversion of **StO** remained low (approximately 30 %) before the increase in molecular weight reached a plateau. The resulting homopolymers **PSt(T)** and **PSt(O)** (Scheme 1) had molecular weights of 11000 g $mol^{-1}$ and 16000 g $mol^{-1}$,

respectively. The number-average degree of polymerization (DPn) was calculated from the gel permeation chromatography

**Table 1** Characterization of **PSt(T)**, **PSt(O)**, **PSt(T-*r*-O)**, **PSt(T-*r*-O-*r*-B)** and **PEG$_{45}$-*b*-PSt(T-*r*-O-*r*-B)s**.

| samples | $DP_n$ (StT)[a] | $DP_n$ (StO)[a] | $DP_n$ (StB)[b] | $M_n$ (GPC) (g mol$^{-1}$)[c] | $M_n$ (NMR) (g mol$^{-1}$)[d] | Đ[c] | LCST (°C)[e] |
|---|---|---|---|---|---|---|---|
| **PSt(T$_{32}$)** | 32 | 0 | 0 | 8900 | - | 1.30 | 19.3 |
| **PSt(O$_{39}$)** | 0 | 39 | 0 | 17500 | - | 1.21 | > 95 |
| **PSt(T$_{24}$-*r*-O$_3$)** | 24 | 3 | 0 | 8200 | - | 1.20 | 34.4 |
| **PSt(T$_{30}$-*r*-StO$_5$)** | 30 | 5 | 0 | 10900 | - | 1.25 | 36.6 |
| **PSt(T$_{39}$- *r* -O$_5$-*r*-B$_{22}$)** | 39 | 5 | 50 | 67300 | 16900 | 1.26 | |
| **PEG$_{45}$-*b*-PSt(T$_{36}$-*r* -B$_{24}$)** | 36 | 0 | 24 | 66000 | 15900 | 1.32 | |
| **PEG$_{45}$-*b*-PSt(T$_{19}$-*r*-O$_3$-*r*-B$_{12}$)** | 19 | 3 | 12 | 57200 | 8800 | 1.26 | |
| **PEG$_{45}$-*b*-PSt(T$_{47}$-*r*-O$_5$-*r*-B$_{10}$)** | 47 | 5 | 10 | 72100 | 19900 | 1.28 | 12.6 |

[a] The number-average degree of polymerization determined by the feed ratio of monomers for copolymerization. [b] The number-average degree of polymerization of **StB** determined by $^1$H NMR integration. [c] A mixture of dimethylformamide (DMF) and dimethylacetamide (DMAc) (99:1 v/v) was used as an eluent with a flow rate of 1 mL/min. [d] The number average molecular weight determined by $^1$H NMR integration. [e] The lower critical solution temperature of the polymer in water (3 mg mL$^{-1}$) determined by turbidity of the solution in UV-Vis spectrometer (absorption at 580 nm).

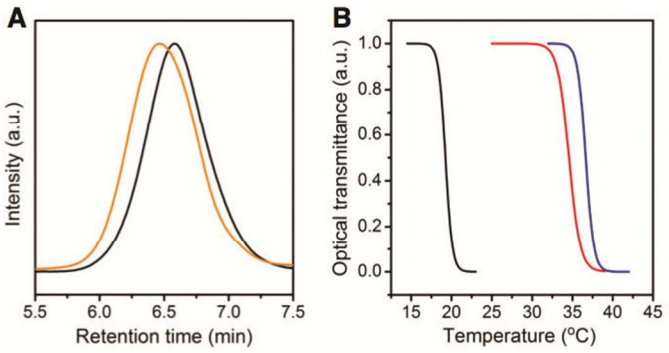


**Figure 2** (A) GPC traces of synthesized **PSt(T)** (black) and **PSt(O)** (orange) (THF, 35 °C). (B) Plots of transmittance as a function of temperature measured for aqueous solutions (3 mg mL$^{-1}$) of **PSt(T)** (black), **PSt(T$_{24}$-*r*-O$_4$)** (red), and **PSt(T$_{30}$-*r*-O$_5$)** (blue). The LCSTs were 19 °C for **PSt(T)**, 34.4 °C for **PSt(T$_{24}$-*r*-O$_4$)**, and 36.6 °C for **PSt(T$_{30}$-*r*-O$_5$)**.

(GPC) results to be 39 for **PSt(T)** and 32 for **PSt(O)** (Table 1) ~~from the GPC results.~~ The GPC results showed well-defined molecular weight and size distributions for both polymers (Figure 2A). **PSt(T)** showed a lower critical solution temperature (LCST) in water of 19 °C (Figure 2B), whereas **PSt(O)** showed an LCST of >95 °C, indicating that these oligo(ethylene glycol)-brushed PS derivatives (OEG-PSs) possessed thermoresponsive behavior in water in an analogous fashion to OEG-polyacrylates.[62-64] By copolymerizing **StT** and **StO**, we controlled the LCST of the resulting OEG-PSs, as shown in Figure 2B. The LCST of the random copolymers **PSt(T$_{24}$-*r*-O$_4$)** and **PSt(T$_{30}$-*r*-O$_5$)** showed a gradual increase as the amount of **StO** used for copolymerization with **StT** was increased. For example, when 13 mol % of **StO** was used for copolymerization with **StT**, the resulting copolymer **PSt(T$_{30}$-*r*-O$_5$)** showed an LCST of 36.6 °C in water. This thermoresponsive behavior of OEG-PSs was analogous to the behavior exhibited by acrylate polymers with pendent OEG groups. To the best of our knowledge, the OEG-PSs described here are the first polystyrene derivatives with tunable LCST in water.

Next, we investigated the effect of the addition of **StB** units onto the OEG-ST backbone on the LCST. We synthesized terpolymers of **StB**, **StT**, and **StO** by RAFT polymerization. The resulting terpolymer **PSt(T$_{39}$-*r*-O$_5$-*r*-B$_{22}$)** possessed 20 mol % of **StB** units in the OEG-ST backbone, which was analysed by $^1$H NMR integration (Figure S3). Despite the presence of water-soluble OEG-ST units as major components of the terpolymer backbone, the terpolymer **PSt(T$_{39}$-*r*-O$_5$-*r*-B$_{22}$)** containing 20 mol % boroxole units in the OEG-ST backbone remained hydrophobic in water at room temperature and reduced temperature (15 °C). These results indicated that the presence of **StB** in the OEG-PS backbone conferred hydrophobicity on the copolymers.

### Synthesis of doubly responsive block copolymers

Given the LCST of OEG-PSs consisting of **StT** and **StO**, we postulated that the OEG-PS backbone of the terpolymers of **StT**, **StO**, and **StB** would be water-soluble, but the glucose-responsive **StB** units in the backbone remained hydrophobic in water at neutral pH within the temperature range of 35~38 °C. Therefore, these terpolymers might exhibit monosaccharide-



 

responsive changes in solubility in water arising from the binding of monosaccharides to benzoboroxole units in aqueous buffer at neutral pH. Based on these assumptions, we

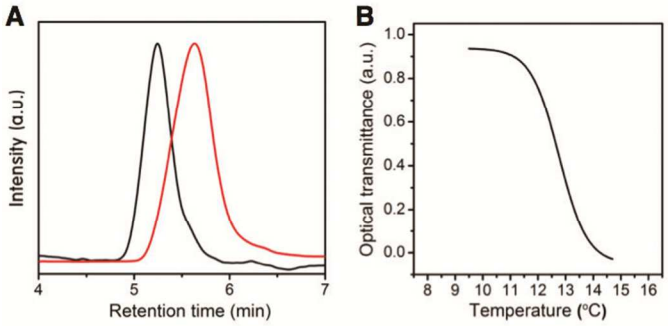


**Figure 3** (A) GPC traces of synthesized block copolymers **PEG$_{45}$-*b*-PSt(T$_{47}$-*r*-O$_5$-*r*-B$_{10}$)** (black) and **PEG$_{45}$-*b*-PSt(T$_{36}$-*r*-B$_{24}$)** (red) (DMF, 65 °C). (B) Plots of transmittance as a function of temperature measured for aqueous solutions (3 mg mL$^{-1}$) of **PEG$_{45}$-*b*-PSt(T$_{47}$-*r*-O$_5$-*r*-B$_{10}$)** (LCST: 12.6 °C).

synthesized the amphiphilic block copolymers **PEG$_{45}$-*b*-PSt(T$_x$-*r*-O$_y$-*r*-B$_z$)** using RAFT polymerization with the poly(ethylene glycol)-chain transfer agent PEG-CTA (Scheme 1). Given the thermoresponsive behavior of the terpolymers described above, we chose the feed ratio of the monomers for copolymerization so that the OEG-ST units provided solubility in water, but the resulting monosaccharide-responsive terpolymer blocks maintained hydrophobicity in water at the temperature range of interest (35~38 °C), in a process which depended on the presence of solubility-switching **StB** units.

$^1$H NMR analysis of the polymerization kinetics indicated first order kinetics and a linear increase in the molecular weight over time, confirming successful RAFT copolymerization. The resulting block copolymers were characterized by $^1$H NMR to quantify the amount of incorporated **StB** units in the backbone, and they were found to have a **StB** content of 8~24 mol % (Figure S4). The GPC results for **PEG$_{45}$-*b*-PSt(T$_x$-*r*-O$_y$-*r*-B$_z$)** showed unimodal peaks with a narrow size distribution ($Đ$ = 1.26-1.33), indicating the successful synthesis of block copolymers with a terpolymer stimuli-responsive block (Figure 3A and Table 1). The resulting block copolymers **PEG$_{45}$-*b*-PSt(T$_x$-*r*-O$_y$-*r*-B$_z$)** were insoluble in water at room temperature, indicating that the presence of the **StB** units conferred hydrophobicity on the resulting stimuli-responsive terpolymer block. However, the block copolymer **PEG$_{45}$-*b*-PSt(T$_{47}$-*r*-O$_5$-*r*-B$_{10}$)**, possessing 8 mol % **StB** content in its OEG-ST backbone exhibited the LCST behavior, with a transition temperature of 12.6 °C (Figure 3B).

### Self-assembly of doubly responsive block copolymers in aqueous solution

The resulting block copolymers **PEG$_{45}$-*b*-PSt(T$_x$-*r*-O$_y$-*r*-B$_z$)** were allowed to self-assemble in water using a co-solvent method. After the addition of water at a controlled rate (2.5 mL h$^{-1}$) to a THF solution of the block copolymers (typically 2 wt %), the resulting cloudy solution was subjected to dialysis against pure water for 24 h to remove the organic solvents. When required, the medium of the suspension was exchanged with buffer (HEPES or PBS, pH 7.5) by centrifugation of the solution and re-dispersion of the concentrate in the buffer. The final concentration of the block copolymers in the solution was adjusted to 0.4 mg mL$^{-1}$.

The resulting suspensions were studied by dynamic light scattering (DLS). For the polymersomes of PEG$_{45}$-*b*-PSt(T$_{36}$-*r*-B$_{24}$), we observed that the self-assembled structures had

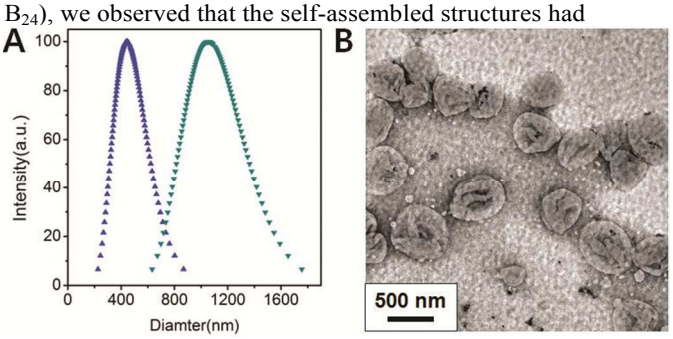


**Figure 4** (A) Size distributions of polymersomes of **PEG$_{45}$-*b*-PSt(T$_{36}$-*r*-B$_{24}$)** (blue) and **PEG$_{45}$-*b*-PSt(T$_{47}$-*r*-O$_5$-*r*-B$_{10}$)** (green) in water. (B) TEM image of polymersomes formed by self-assembly of **PEG$_{45}$-*b*-PSt(T$_{36}$-*r*-B$_{24}$)** in water.

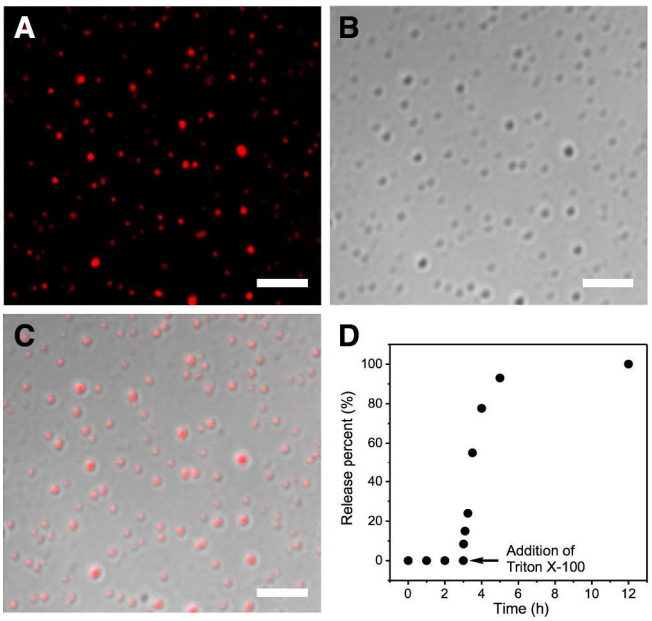


**Figure 5** CLSM images of polymersomes of **PEG$_{45}$-*b*-PSt(T$_{47}$-*r*-O$_5$-*r*-B$_{10}$)** encapsulating Rhodamine B dyes. (A) Dark-field, (B) Bright-field; (C) Merged. Scale bars: 5 μm. (D) Release profile of Rhodamine B from polymersome of **PEG$_{45}$-*b*-PSt(T$_{47}$-*r*-O$_5$-*r*-B$_{10}$)**.

~~average~~ diameters of 200~400 nm with a moderate polydispersity (~ 0.3) (Figure 4A). We assessed the morphology of the self-assembled structures by inspecting the dried solution using transmission electron microscopy (TEM). In all cases, we observed polymer vesicles (polymersomes) with diameters ranging from 200 to 450 nm, which confirmed the DLS results (Figure 4A and Figure S5). For the polymersome solutions of **PEG$_{45}$-*b*-PSt(T$_{36}$-*r*-B$_{24}$)** and **PEG$_{45}$-*b*-PSt(T$_{47}$-*r*-O$_5$-*r*-B$_{10}$)** in aqueous buffer at neutral pH, we observed no changes in the scattered light intensity or average diameter at room temperature over a 1 week period, which indicated that the polymersomes of **PEG$_{45}$-*b*-PSt(T$_{36}$-*r*-B$_{24}$)** and **PEG$_{45}$-*b*-PSt(T$_{47}$-*r*-O$_5$-*r*-B$_{10}$)** maintained their structural integrity in aqueous solution at neutral pH for an extended period of time (~ 1 week) (Figure S6). In contrast, the polymersome solution of **PEG$_{45}$-*b*-PSt(T$_{19}$-*r*-O$_3$-*r*-B$_{12}$)**, having the stimuli-responsive terpolymer block with the smallest

molecular weight of the tested block copolymers, showed a gradual decrease in turbidity over the 1 week in aqueous buffer (pH 7.5), suggesting that the polymersomes of this block copolymer lacked structural stability over time. Therefore, we used the block copolymer **PEG$_{45}$-*b*-PSt(T$_{36}$-*r*-B$_{24}$)** and **PEG$_{45}$-*b*-PSt(T$_{47}$-*r*-O$_5$-*r*-B$_{10}$)** for further characterizations and investigations.

To demonstrate the ability of the polymersomes to carry water-soluble cargo molecules within their inner compartments, we encapsulated Rhodamine B within the polymersomes by adding water containing the fluorescent dye (0.5 mg mL$^{-1}$) to a THF solution of the block copolymer **PEG$_{45}$-*b*-PSt(T$_{47}$-*r*-O$_5$-*r*-B$_{10}$)**. The resulting suspension was purified by dialysis and size exclusion chromatography (Sephadex G-100) to remove unencapsulated dye from the polymersome solution. The measured loading efficiency of Rhodamine B was 23 %, and the content of Rhodamine B encapsulated within the polymersomes was 1.17 %. The purified polymersome solution was examined by confocal laser scanning microscopy (CLSM) (Figure 5A-C). The encapsulated molecules were well contained within the water-filled inner compartment of the polymersomes, showing strong fluorescence centered on the lumen of the polymersome, as visualized by CLSM at 11 different focal planes (Figure S7). The polymersomes of **PEG$_{45}$-*b*-PSt(T$_{47}$-*r*-O$_5$-*r*-B$_{10}$)** encapsulating Rhodamine B retained their structural integrity in water over 20 days, showing no decrease in fluorescence intensity (Figure S8). The hollow structure of the polymersomes was disrupted by adding Triton X-100, a surfactant routinely used to lyse polymers and cellular membranes (Figure 5D).[65] Upon the addition of Triton X-100 to the polymersome solution of **PEG$_{45}$-*b*-PSt(T$_{47}$-*r*-O$_5$-*r*-B$_{10}$)**, the water-soluble Rhodamine B entrapped in the water-filled compartments of the polymersomes were suddenly released within 2 h, due to disruption of the polymer membranes by Triton X-100. This result indicated the release of the dye contained within the inner compartment of the polymersomes, resulting in the diminished frequency of the quenching of the fluorescence of the dye molecules.

### Stimuli-responsive disassembly of polymersomes

The monosaccharide-responsive behavior of boroxole-containing polymers arises from the binding of a monosaccharide to a benzoboroxole unit, conferring a negative charge at the tetravalent boron center and resulting in the additional hydroxyl groups of the monosaccharide bound to the polymers. In this case of the polymers containing monosaccharide-responsive boroxole group, the benzoboroxole unit serves as a switch to change the solubility of the boroxole-containing polymers in water. We conjectured that the number of benzoboroxole units in the polymer backbone could be minimized by adopting the water-soluble repeat units as a major structural component. By using a minimum number of solubility-switching boroxole units in the hydrophilic polymer backbone, changes in the solubility of the resulting polymers and block copolymers in water could be triggered at a low concentration of monosaccharides in solution.

To prove our hypothesis, we introduced a co-monomer with a water-compatible moiety, N-functionalized maleimides with oligo(ethylene glycol) groups, to perform the alternating co-polymerization with **StB**. This polymerization yielded the copolymers, in which the glucose-responsive **StB** unit alternated with non-responsive maleimide units with a solubilizing group.[61] Due to the presence of solubilizing groups surrounding the glucose-responsive boroxole units in the polymer backbone, the resulting copolymers showed glucose-responsive behavior at a glucose concentration lower than that required to produce glucose-responsive behavior in PBOx homopolymers.

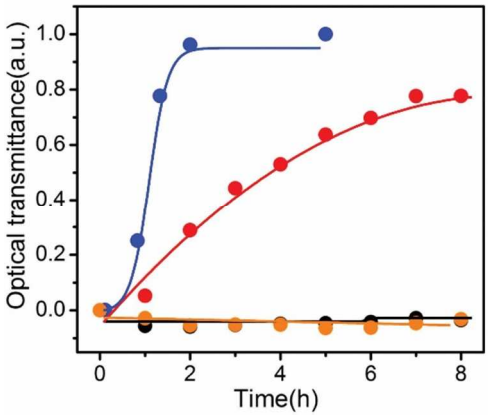


**Figure 6** Temperature dependency of optical transmittance profiles of the polymersome solution of **PEG$_{45}$-*b*-PSt(T$_{36}$-*r*-B$_{24}$)** in the absence (orange dots at 17 °C and black dots at 37 °C) and the presence of fructose (0.05 M) at 17 °C (blue dots) and 37 °C (red dots) (HEPES pH 7.5).

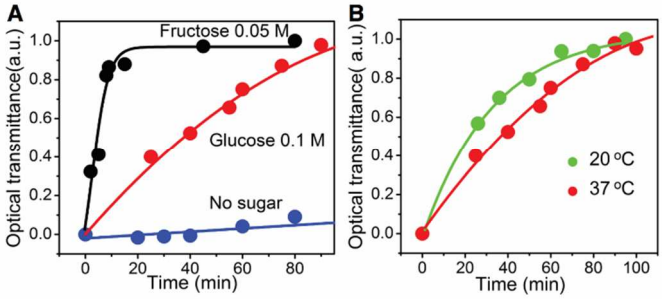


**Figure 7** (A) Optical transmittance profiles of the polymersome solution of **PEG$_{45}$-*b*-PSt(T$_{47}$-*r*-O$_5$-*r*-B$_{10}$)** in the presence of monosaccharides (37 °C, HEPES pH 7.5). (B) Temperature dependency of optical transmittance profiles of the polymersome solution of **PEG$_{45}$-*b*-PSt(T$_{47}$-*r*-O$_5$-*r*-B$_{10}$)** in the presence of glucose (0.1 M in HEPES pH 7.5).

The terpolymer block consisting of OEG-STs and **StB** exhibited a solubility change in water upon binding of monosaccharides to the benzoboroxole group on the polymer backbone. When the stimuli-responsive terpolymer containing block copolymers self-assembled into the bilayers constructing the polymersomes, the resulting polymersomes showed stimuli-responsive disassembly in water at neutral pH in response to the presence of monosaccharides. The monosaccharide-responsive disassembly behavior of the polymersomes of **PEG$_{45}$-*b*-PSt(T$_{36}$-*r*-B$_{24}$)** and **PEG$_{45}$-*b*-PSt(T$_{47}$-*r*-O$_5$-*r*-B$_{10}$)** was studied by measuring changes in the turbidity of the polymersome solution. At 37 °C, the polymersome of **PEG$_{45}$-*b*-PSt(T$_{36}$-*r*-B$_{24}$)** in HEPES buffer (pH 7.5) showed monosaccharide-responsive disassembly in the presence of 0.05 M fructose (Figure 6). We measured the response time for the disassembly of polymersomes by measuring $t_R$, which was defined as the time required to reach 50% of transmittance at 580 nm at a given monosaccharide concentration. The $t_R$ of the

polymersomes of **PEG$_{45}$-*b*-PSt(T$_{36}$-*r*-B$_{24}$)** at 37 °C was 3.5 h for fructose (0.05 M) (Figure 6).

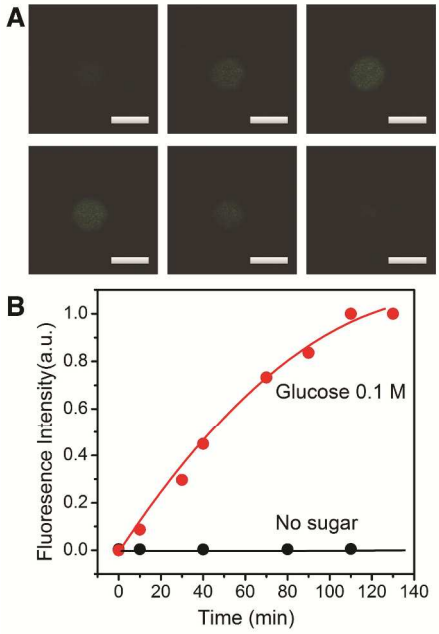


**Figure 8** (A) CLSM images of polymersome of **PEG$_{45}$-*b*-PSt(T$_{47}$-*r*-O$_5$-*r*-B$_{10}$)** encapsulating F-insulin at 6 different focal planes. Scale bar: 2 μm. (B) Release profiles of insulin from the polymersomes of **PEG$_{45}$-*b*-PSt(T$_{47}$-*r*-O$_5$-*r*-B$_{10}$)** in HEPES buffer (pH 7.5).

Upon decreasing the temperature of the solution to 17 °C, the $t_R$ of the polymersome solution of **PEG$_{45}$-*b*-PSt(T$_{36}$-*r*-B$_{24}$)** was reduced to 1 h for 0.05 M fructose (Figure 6). This enhanced responsive behavior of the polymersome of **PEG$_{45}$-*b*-PSt(T$_{36}$-*r*-B$_{24}$)** toward monosaccharides at lower temperature was believed to be due to the increased water-solubility of the OEG moieties in the polymer backbone due to the LCST behavior of OEG-STs.

Given the monosaccharide-responsive behavior of the polymersomes of **PEG$_{45}$-*b*-PSt(T$_{36}$-*r*-B$_{24}$)** in aqueous buffer at neutral pH, we expected that the polymersomes consisting of the block copolymer **PEG$_{45}$-*b*-PSt(T$_{47}$-*r*-O$_5$-*r*-B$_{10}$)** would show enhanced responsiveness toward monosaccharides due to the reduced number of **StB** units in the responsive block in comparison with the terpolymer block of **PEG$_{45}$-*b*-PSt(T$_{36}$-*r*-B$_{24}$)**. Therefore, we measured the turbidity of the polymersome solution of **PEG$_{45}$-*b*-PSt(T$_{47}$-*r*-O$_5$-*r*-B$_{10}$)** in aqueous buffer at neutral pH in the presence of monosaccharides at 37 °C. The polymersome solution of **PEG$_{45}$-*b*-PSt(T$_{47}$-*r*-O$_5$-*r*-B$_{10}$)** in HEPES buffer (pH 7.5) showed monosaccharide-triggered disassembly behaviors in the presence of fructose (0.05 M) and glucose (0.1 M) at 37 °C (Figure 7A), and the $t_R$ was determined to be 5 min for 0.05 M fructose and 40 min for 0.1 M glucose, which were significantly shorter response times than those of the polymersome solutions of **PEG$_{45}$-*b*-PSt(T$_{36}$-*r*-B$_{24}$)**.[60] These results indicated that the reduced number of solubility-switching **StB** units in the responsive terpolymer backbone enhanced disassembly of the self-assembled block copolymer bilayer comprising the polymersomes in the presence of a lower concentration of monosaccharides in solution. We also investigated the effect of temperature on the disassembly behavior of the polymersome of **PEG$_{45}$-*b*-PSt(T$_{47}$-*r*-O$_5$-*r*-B$_{10}$)**. When the temperature of the solution was decreased to 20 °C, the $t_R$ of the polymersome solution of **PEG$_{45}$-*b*-PSt(T$_{47}$-*r*-O$_5$-*r*-B$_{10}$)** was decreased to 22 min for 0.1 M glucose, whereas the $t_R$ at 37 °C was 40 min (Figure 7B). This sugar-responsive behavior of polymersomes of **PEG$_{45}$-*b*-PSt(T$_{47}$-*r*-O$_5$-*r*-B$_{10}$)** in the presence of glucose (0.1 M) was further corroborated from the disappearance of polymersomes at different temperatures in the DLS study (Figure S9). These results demonstrated that the enhanced water-solubility of the OEG-ST backbone containing solubility-switching benzoboroxole units enhanced responsiveness of the terpolymer block toward monosaccharides in solution. This enhanced responsive behavior of the terpolymer block might be arisen from the increase in the chance of binding of monosaccharide to **StB** units by enhancing the diffusion of sugar molecules through the swollen bilayer membrane consisting mostly of water-soluble OEG-ST units below the LCST of the polymer backbone.

Judging from the low cytotoxicity of **PEG$_{45}$-*b*-PSt(T$_{47}$-*r*-O$_5$-*r*-B$_{10}$)** having high cell viability (>90 % of HeLa cells at 3 mg/mL), we assessed the monosaccharide-responsive release behavior of the polymersomes of **PEG$_{45}$-*b*-PSt(T$_{47}$-*r*-O$_5$-*r*-B$_{10}$)** encapsulating fluorescein isothiocyanate (FITC)-labeled human insulin (F-insulin) (see ESI).[60,61] As shown in Figure 8A, CLSM analysis revealed the successful loading of F-insulin within the polymersome of **PEG$_{45}$-*b*-PSt(T$_{47}$-*r*-O$_5$-*r*-B$_{10}$)**, which was stable in HEPES solution (pH 7.5) without leakage of F-insulin (Figure 8B). In sharp contrast, encapsulated F-insulin was released from the polymersomes in response to the presence of glucose (Figure 8B).

## Conclusions

We studied doubly responsive terpolymers consisting of OEG-STs and **StB**, which were polymerized under RAFT conditions. The oligo (ethylene glycol) groups tethered to the polymer backbone conferred thermally responsive behavior on the resulting polymers, as evidenced by their tunable LCST behavior. The styrene-boroxole units introduced to the terpolymers were responsible for the monosaccharide-responsive changes in polymer solubility in water. Combining these responsive behaviors, we synthesized block copolymers, **PEG$_{45}$-*b*-PSt(T$_x$-*r*-O$_y$-*r*-B$_z$)**, that self-assembled into polymersomes in aqueous solution. The resulting polymersomes were capable of encapsulating water-soluble cargo molecules within their inner compartments, and showed monosaccharide responsive disassembly in water, by which the encapsulated guest molecules were released in response to the presence of glucose and fructose in the medium. By utilizing the tunable thermoresponsive behavior of the OEG-ST backbone, we optimized the hydrophobicity of the terpolymer by adjusting the amount of **StB** introduced for copolymerization. At the temperature range of interest (~37 °C), OEG-ST units provided water-compatibility to the responsive terpolymer block, while the change in solubility relied on the binding of monosaccharides to the benzoboroxole group of **StB**. We showed that these doubly responsive polymersomes exhibited enhanced responsiveness toward monosaccharides such as glucose and fructose at 37 °C in comparison with that of polymersosomes built from block copolymers with a homopolymer of **StB** as a responsive block. Moreover, the polymersomes of **PEG$_{45}$-*b*-PSt(T$_x$-*r*-O$_y$-*r*-B$_z$)s** showed an enhanced rate of disassembly in the presence of monosaccharides at a lower temperature, which indicated that the thermoresponsive nature of the terpolymer block was responsible for the enhanced responsiveness of the

polymersomes toward monosaccharides. These doubly responsive block copolymers reported herein, which are responsive to multiple stimuli, could be utilized in the development of smart delivery vehicles capable of self-regulating the release of encapsulated molecules ~~in complex~~ in vivo environments.

## Acknowledgements

This research was supported by National Research Foundation (NRF) of Korea (NRF-2013R1A1A013075) and UNIST (UMI future challenge grant). C.P. acknowledges NRF for the research fellowship (2013R1A1A2063049). We thank UCRF and UOBC for microscopy facilities. We thank M. G. Jeong and Y. La for their help with illustration and optical microscopy.

## Notes and references

[a] Department of Chemistry, Ulsan National Institute of Science and Technology (UNIST), 50 UNIST Road, Ulsan 689-798, Korea
Email: cpark@unist.ac.kr, ktkim@unist.ac.kr

† Electronic Supplementary Information (ESI) available: [Materials, instrumentation, experimental details, synthetic procedures, characterization data of block copolymers, and additional electron microscopy images]. See DOI: 10.1039/b000000x/

1 Hamley, I. W. *Block Copolymers in Solution: Fundamentals and Applications*, Wiley 2005 (Chichester).

2 (a) P. Tanner, P. Baumann, R. Enea, O. Onaca, C. Palivan and W. Meier, *Acc. Chem. Res.* 2011, **44**, 1039-1049. (b) G. Yu, K. Jie, and F. Huang, *Chem. Rev*,2015,**115**, DOI: 10.1021/cr5005315. (c) X. Ji, J. Li, J. Chen, X. Chi, K. Zhu, X. Yan, M.Zhang, and F.Huang, *Macromolecules,* 2012, **45**, 6457−6463. (d) X. Ji , S. Dong , P. Wei , D. Xia , and F. Huang, *Adv. Mater*. 2013, **25**, 5725–5729.

3 F. Meng and Z. Zhong, *J. Phys. Chem. Lett*. 2011, **2**, 1533-1539.

4 (a) A. Rösler, G. W. M. Vandermeulen and H.-A. Klok, *Adv. Drug Delivery Rev.* 2012, **64**, 270-279. (b) X. Chi, X. Ji, D. Xia, and F. Huang, *J. Am. Chem. Soc*. 2015, **137**, 1440−1443.

5 R. P. Brinkhuis, F. P. J. T. Rutjes and J. C. M. van Hest, *Polym. Chem*. 2011, **2**, 1449-1462.

6 F. Meng, Z. Zhong, and J. Feijen, *Biomacromolecules* 2009, **10**, 197-209.

7 M.-H. Li, and P. Keller, *Soft Matter* 2009, **5**, 927-937.

8 E. Mabrouk, D. Cuvelier, F. Brochard-Wyart, P. Nassoy, and M.-H. Li, *Proc. Natl. Acad. Sci. U.S.A.* 2009, **106**, 7294-7298.

9 S. Yu, T. Azzam, I. Roulier and A. Eisenberg, *J. Am. Chem. Soc*. 2009, **131**, 10557-10566.

10 F. Ahmed, R. I. Pakunlu, A. Brannan, F. Bates, T. Minko and D. E. Discher, *J. Controlled Release* 2006, **116**, 150-158.

11 E. G. Bellomo, M. D. Wyrsta, L. Pakstis, D. J. Pochan and T. J. Deming, *Nat. Mater*. 2004, **3**, 244-248.

12 G. P. Robbins, M. Jimbo, J. Swift, M. J. Therien, D. A. Hammer and I. J. Dmochowski, *J. Am. Chem. Soc*. 2009, **131**, 3872-3874.

13 Q. Wu, L. Wang, H. Yu, J. Wang and Z. Chen, *Chem. Rev*. 2011, **111**, 7855-7875.

14 A. W. Du and M. H. Stenzel, *Biomacromolecules* 2014, **15**, 1097-1114.

15 R. Mo, T. Jiang, J. Di, W. Tai and Z. Gu, *Chem. Soc. Rev.* 2014, **43**, 3595-3629.

16 M. Elsabahy and K. L. Wooley, *Chem. Soc. Rev*. 2012, **41**, 2545-2561.

17 X. Yan, F. Wang, B. Zheng and F. Huan, *Chem. Soc. Rev*. 2012, **41**, 6042-6065.

18 S. Dong, Y. Luo, X. Yan, B. Zheng, X. Ding, Y. Yu,. Z. Ma, Q. Zhao and F. Huang, *Angew. Chem. Int. Ed*. 2011, **50**, 1905-1909.

19 H. P. James, R. John, A. Alex and K. R. Anoop, *Acta Pharm. Sin. B*. 2014, **4**,120-127.

20 D. Peer,J. M. Karp, S. Hong, O. C. Farokhzad, R. Margalit and R. Langer, *Nat. Nanotech*. 2007, **2**, 751-760.

21 J. Shi, A. R. Votruba, O. C. Farokhzad and R. Langer, *Nano Lett*., 2010, **10**, 3223-3230.

22 W. Tai, R. Mo, J. Di, V. Subramanian, X. Gu, J. B. Buse and Z. Gu, *Biomacromolecules* 2014, **15**, 3495-3502.

23 W. Yuan, T. Shen, J. Wang and H. Zou, *Polym. Chem*. 2014, **5**, 3968-3971.

24 I. Tokarev and S. Minko, *Adv. Mater.* 2009, **21**, 241-247.

25 S. Mura, J. Nicolas and P. Couvreur, *Nature Mater*. 2013, **12**, 991-1003.

26 R. Nishiyabu, Y. Kubo, T. D. James and J. S. Fossey, *Chem. Commun*. 2011, **47**, 1106-1123.

27 J. N. Cambre and B. S. Sumerlin, *Polymer* 2011, **52**, 4631-4984.

28 F. Cheng and F. Jäkle, *Polym. Chem*. 2011, **2**, 2122-2132.

29 F. Jäkle, *Chem. Rev*. 2010, **110**, 3985-4022.

30 Y. Qin, V. Sukul, D. Pagakos, C. Cui and F. Jäkle, *Macromolecules* 2005, **38**, 8987-8990.

31 Y. Kanekiyo, M. Sano, R. Iguchi and S. Shinkai, *J. Polym. Sci., Part A: Polym. Chem*. 2000, **38**, 1302-1310.

32 K. Kataoka, H. Miyazaki, M. Bunya, T. Okano and Y. Sakurai, *J. Am. Chem. Soc.* 1998, **120**, 12694-12695.

33 A. Matsumoto, R. Yoshida and K. Kataoka, *Biomacromolecules* 2004, **5**, 1038-1045.

34 A. Matsumoto, K. Yamamoto, R. Yoshida, K. Kataoka, T. Aoyagi and Y. Miyahara, *Chem. Commun*. 2010, **46**, 2203-2205.

35 Y. E. Aguirre-Chagala, J. L. Santos, B. A. Aguilar-Castillo, M. Herrera-Alonso, *ACS Macro Lett*. 2014, **3**, 353-358.

36 Y. E. Auirre-Chagala, J. L. Santos, Y. Huang and M. Herrera-Alonso, *ACS Macro Lett*. 2014, **3**, 1249-1253.

37 J. Ye, Y. Chen and Z. Liu, *Angew. Chem. Int. Ed.* 2014, **53**, 10386-10389.

38 L. Li, Y. Lu, Z. Bie, H.-Y. Chen, Z. Liu, *Angew. Chem. Int. Ed*. 2013, **52**, 7451-7454.

39 M. Elstner, J. Axthelm and A. Schiller, *Angew. Chem. Int. Ed*. 2014, **53**, 7339-7343.

40 M. Zhou, J. Xie, S. Yan, X. Jiang, T. Ye and W. Wu, *Macromolecules* 2014, **47**, 6055-6066.

41 S. Wang, J. Ye, Z. Bie and Z. Liu, *Chem. Sci*. 2014, **5**, 1135-1140.

42 S. Chantasirichot, Y. Inoue and K. Ishihara, *Macromolecules* 2014, **47**, 3128-3135.

43 Y. Kotsuchibashi, R. V. C. Agustin, J.-Y. Lu, D. G. Hall and R. Narain, *ACS Macro Lett*. 2013, **2**, 260-264.

44 J. Zhang, M. P. Landry, P. W. Barone, J.-H. Kim, S. Lin, Z. W. Ulissi, D. Lin, B. Mu, A. A. Boghossian, A. J. Hilmer, A. Rwei, A. C. Hinckely, S. Kruss, M. A. Shandell, N. Nair, S. Blake, F. Sen, R.



 

G. Croy, D. Li, K. Yum, J.-H. Ahn, H. Jin, D. A. Heller, J. M. Essigmann, D. Blankschtein and M. S. Strano. *Nat. Nanotech*. 2013, **8**, 959-968.

45 Z. Gu, A. A. Aimetti, Q. Wang, T. T. Dang, Y. Zhang, O. Veiseh, H. Cheng, R. Langer and D. G. Anderson, *ACS Nano* 2013, **7**, 4194-4201.

46 Z. Gu, T. T. Dang, M. Ma, B. C. Tang, H. Cheng, S. Jiang, Y. Dong, Y. Zhang and D. G. Anderson, *ACS Nano* 2013, **7**, 6758-6766.

47 T. Yang, R. Ji, X.-X. Deng, F.-S. Du and Z. Li, *Soft Matter* 2014, **10**, 2671-2678.

48 M. Nakahata, S. Mori, Y. Takashima, A. Hashidzume, H. Yamaguchi and A. Harada, *ACS Macro Lett*. 2014, **3**, 337-340.

49 T. D. James and S. Shinkai, *Top. Curr. Chem.* 2002, **218**, 159-200.

50 T. D. Janmes, K. R. A. S. Sandanayake and S. Shinkai, *Angew. Chem., Int. Ed.* 1996, **35**, 1910-1922.

51 N. Fujita, S. Shinkai and T. D. James, *Chem. Asian. J*. 2008, **3**, 1076-1091.

52 M. Dowlut and D. G. Hall, *J. Am. Chem. Soc*. 2006, **128**, 4226-4227.

53 M. Bérubé, M. Dowlut and D. G. Hall, *J. Org. Chem*. 2008, **73**, 6471-6479.

54 J. W. Tomsho, A. Pal, D. G. Hall and S. J. Benkovic, *ACS Med. Chem. Lett*. 2012, **3**, 48-52.

55 J. N. Cambre, D. Roy, S. R. Gondi and B. S. Sumerlin, *J. Am. Chem. Soc*. 2007, **129**, 10348-10349.

56 D. Roy, J. N. Cambre and B. S. Sumerlin, *Chem. Commun*. 2008, 2477-2479.

57 K. T. Kim, J. J. L. M. Cornelissen, R. J. M. Nolte and J. C. M. van Hest, *Adv. Mater*. 2009, **21**, 2787-2791.

58 A. P. Bapat, D. Roy, J. G. Ray, D. A. Savin and B. S. Sumerlin, *J. Am. Chem. Soc.* 2011, **133**, 19832-19838.

59 K. T. Kim, J. J. L. M. Cornelissen, R. J. M. Nolte and J. C. M. van Hest, *J. Am. Chem. Soc*. 2009, **131**, 13908-13909.

60 H. Kim, Y. J. Kang, S. Kang and K. T. Kim, *J. Am. Chem. Soc.* 2012, **134**, 4030-4033.

61 H. Kim, Y. J. Kang, E. S. Jeong, S. Kang and K. T. Kim, *ACS Macro Lett.* 2012, **1**, 1194-1198.

62 J.-F. Lutz, Ö. Akdemir and A. Hoth, *J. Am. Chem. Soc.* 2006, **128**, 13046-13047.

63 J.-F. Lutz, *J. Polym. Sci., Part A: Polym. Chem*. 2008, **46**, 3459-3470.

64 G. B. H. Chua, P. J. Roth, H. T. T. Duong, T. P. Davis, A. B. Lowe, *Macromolecules* 2012, **45**, 1362-1374.

65 N. P. Kamat, Z. Liao, L. E. Moses, J. Rawson, M. J. Therien, I. J. Dmochowski and D. A. Hammer, *Proc. Natl. Acad. Sci. U.S.A*. 2011, **108**, 13984-13989.